

---

# On Deep Domain Adaptation: Some Theoretical Understandings

---

Trung Le, Khanh Nguyen, Nhat Ho, Hung Bui, Dinh Phung

## Abstract

Compared with shallow domain adaptation, recent progress in deep domain adaptation has shown that it can achieve higher predictive performance and stronger capacity to tackle structural data (e.g., image and sequential data). The underlying idea of deep domain adaptation is to bridge the gap between source and target domains in a joint space so that a supervised classifier trained on labeled source data can be nicely transferred to the target domain. This idea is certainly intuitive and powerful, however, limited theoretical understandings have been developed to support its underpinning principle. In this paper, we have provided a rigorous framework to explain why it is possible to close the gap of the target and source domains in the joint space. More specifically, we first study the loss incurred when performing transfer learning from the source to the target domain. This provides a theory that explains and generalizes existing work in deep domain adaptation which was mainly empirical. This enables us to further explain why closing the gap in the joint space can directly minimize the loss incurred for transfer learning between the two domains. To our knowledge, this offers the first theoretical result that characterizes a direct bound on the joint space and the gain of transfer learning via deep domain adaptation.

## 1 Introduction

Learning a discriminative classifier or other predictor in the presence of a shift between source (training) and target (testing) distributions is known as domain adaptation (DA). Domain adaptation aims to devise automatic methods that make it possible to perform transfer learning from the source domain with labels to the target domains without labels. Studies in domain adaptation can be broadly categorized into two themes: shallow and deep domain adaptations. A number of approaches to domain adaptation have been suggested in the context of shallow learning when data representations/features are given and fixed, notably via reweighing or selecting samples from the source domain [3, 11, 7] or seeking an explicit feature space transformation that would map source distribution into the target ones [17, 9, 1].

To further advance shallow domain adaptation, deep domain adaptation has recently been proposed to encourage the learning of new representations for both source and target data in order to minimize the divergence between them [6, 21, 13, 14, 19, 5]. Source and target data are mapped to a joint feature space via a generator and the gap between source and target distributions is bridged in this joint space by minimizing the divergence between distributions induced from the source and target domains on this space. For instance, the works of [6, 21, 13, 19, 5] minimize the Jensen-Shannon divergence between the two relevant distributions relying on GAN principle [8], while the work of [13] minimizes the maximum mean discrepancy (MMD) [10] and the work of [4] minimizes the Wasserstein distance between them. The idea of bridging the gap of the source and target domains in a joint feature space is an intuitive and powerful one. However, to our best of knowledge, there is limited theoretical work has been proposed to rigorously explain and provide a theoretical underpinning for this problem.

Some existing work has attempted to study this problem, notably [15, 2, 18, 23]. The works of [2, 18] assumed the existence of a common hypothesis space used for both source and target domains and then performed theoretical analysis under this assumption which might be unrealistic in real-world scenarios. In particular, the work of [2] analyzed for the specific loss function  $|h(\mathbf{x}) - f(\mathbf{x})|$  (i.e., 0 – 1 loss) and its Theorem 1 indicates the target error can be bounded by the sum of the source error, the total variance distance between the source and target domains, and the discrepancy between the labeling assignment distributions of the source and target domains. The work of [18] studied for the loss function  $|h(\mathbf{x}) - f(\mathbf{x})|^q$ , but its result fails to capture the discrepancy between the labeling assignment distributions of the source and target domains, which, as shown in our experiments, is important for the transfer learning performance.

In this paper, we aim to develop a rigorous framework to study the deep domain adaptation problem. Unlike [2, 18], we do not assume that the hypothesis spaces for the source and target domains are the same. More specifically, the hypothesis spaces for the target and source domains are shifted by a transformation  $T_{ts}$ . Furthermore, our results also hold for any continuous loss function satisfying a mild condition and is analyzed under a general setting of having a probabilistic supervisor that assigns labels to data examples [22]. Under these much more general conditions than [2], we are still able to generalize the result in [2] to show that the gap between general losses of two corresponding hypotheses over the source and target domains is upper-bounded by the Wasserstein distance between the source distribution and the pushforward distribution of the target distribution via the transformation  $T_{ts}$  plus an additional discrepancy between the two label assignment distributions on the two domains.

This result leads us to learn a bijective transformation  $T_{ts}$  that minimizes the WS distance between the source distribution and the induced distribution of the target distribution via  $T_{ts}$ . This minimization step further sheds light on the need to close the gap between the source and target distributions in a joint space and provides a rigorous underlying explanation for the success in most of current existing empirical deep domain adaptation work. Moreover, the theory also indicates that by minimizing the first term (i.e., the Wasserstein distance term), we could accidentally increase the second term (i.e., the discrepancy between two labeling assignment mechanisms), hence possibly eventually increasing the relevant upper bound. We conduct the extensive experiments on the synthetic and real-world datasets to verify the theoretical results obtained and to study the behaviors when the transport transformation  $T_{ts}$  causes the total/partial match or mismatch of two labeling assignment mechanisms in the joint space. Last but not least, our result has a strong implication to unsupervised style transfer (e.g., CycleGAN [24] and DiscoGAN [12]) in which one needs to learn a non-degenerate map that transports the source to target distributions. Interestingly, our proposed theory can be used to theoretically explain the formulation of CycleGAN and DiscoGAN, hence it contributes to deepen the understanding of these popular models in unsupervised style transfer.

## 2 Main Results

To facilitate the presentation later, we assume that the data spaces of the source and target domains are  $\mathcal{X}^s$  and  $\mathcal{X}^t$  respectively. Furthermore, we denote the distributions that generate data samples for the source and target domains as  $p^s(\mathbf{x})$  (corresponding to the probability measure  $\mathbb{P}^s$ ) and  $p^t(\mathbf{x})$  (corresponding to the probability measure  $\mathbb{P}^t$ ) respectively. We also denote the supervisor distributions that assign labels to data samples in the source and target domains as  $p^s(y | \mathbf{x})$  and  $p^t(y | \mathbf{x})$  [22].

Denote by  $\mathcal{H}^s := \{h^s : \mathcal{X}^s \rightarrow \mathbb{R}\}$  the hypothesis set whose elements are used to predict labels source data. Throughout this paper, we assume that  $T_{ts} : \mathcal{X}^t \rightarrow \mathcal{X}^s$  is a *bijective* mapping and  $T_{st} := T_{ts}^{-1}$  is the inverse of  $T_{ts}$ . Based on the formulation of hypothesis set  $\mathcal{H}^s$ , we define hypothesis set for target domain as  $\mathcal{H}^t := \{h^t : \mathcal{X}^t \rightarrow \mathbb{R} \mid h^t(\cdot) = h^s(T_{ts}(\cdot)) \text{ for some } h^s \in \mathcal{H}^s\}$ .

The intuition behind these definitions and assumptions is that with  $\mathbf{x} \sim \mathbb{P}^t$ , we use the mapping  $T_{ts}$  to reduce the difference between two domains and then apply a hypothesis  $h^s \in \mathcal{H}^s$  to predict the label of  $\mathbf{x}$ . This gives rise to the question about the key properties of the transformation mapping  $T_{ts}$  so that we can employ the hypothesis  $h^t = h^s \circ T_{ts}$  to predict labels of target data where  $\circ$  represents the composition function.

Now, we define by  $P^\# := (T_{ts})_\# \mathbb{P}^t$  the pushforward probability distribution induced by transporting  $\mathbb{P}^t$  via  $T_{ts}$ . Then, we denote  $p^\#(\mathbf{x})$  the density of the probability distribution  $P^\#$ . It induces a new

domain, which is termed as the *transport domain* whose data are generated from  $\mathbb{P}^\#$ . Given these definitions, we define the supervisor distribution for the transport domain as  $p^\#(y | \mathbf{x}) = p^t(y | \mathbf{x}^t)$  where  $\mathbf{x}^t = T_{ts}^{-1}(\mathbf{x}) = T_{st}(\mathbf{x})$  for any  $\mathbf{x} \in \mathcal{X}^s$ . To ease the presentation, we denote the general expected loss as:

$$R^{a,b}(h) := \int \ell(y, h(\mathbf{x})) p^b(y | \mathbf{x}) p^a(\mathbf{x}) d\mathbf{x},$$

where  $a, b$  are in the set  $\{s, t, \#\}$  and  $\ell(\cdot, \cdot)$  specifies a loss function. In addition, we shorten  $R^{a,a}$  as  $R^a$ . Furthermore, given a hypothesis  $h^s \in \mathcal{H}^s$  and  $h^t = h^s \circ T_{ts}$ , we measure the variance of general losses of  $h^s$  when predicting on the source domain and general losses of  $h^t$  when predicting on the target domain as:

$$\Delta R(h^s, h^t) := |R^t(h^t) - R^s(h^s)|.$$

Finally, for the simplicity of the results in the paper, we consider solely the case of binary classification where the label  $y \in \{-1, 1\}$ . Please refer to our supplementary material for the relevant background and the details of all proof.

## 2.1 Gap between target and source domains

In this subsection, we investigate the variance  $\Delta R(h^s, h^t)$  between the expected loss in target domain  $R^t(h^t)$  and the expected loss in source domain  $R^s(h^s)$  where  $h^t = h^s \circ T_{ts}$ . We embark on with the following simple yet key proposition indicating the connection between  $R^t(h^t)$  and  $R^\#(h^s)$ .

**Proposition 1.** *As long as  $h^t = h^s \circ T_{ts}$ , we have  $R^t(h^t) = R^\#(h^s)$ .*

To derive a relation between  $R^t(h^t)$  and  $R^s(h^s)$ , we make the following mild assumption with loss function  $\ell$ :

$$(A.1) \sup_{h^s \in \mathcal{H}^s, \mathbf{x} \in \mathcal{X}^s, y \in \{-1, 1\}} |\ell(y, h^s(\mathbf{x}))| := M < \infty.$$

With simple algebra manipulation, the above assumption is satisfied when  $\ell$  is a bounded loss, e.g., logistic or 0-1 loss or  $\ell$  is any continuous loss,  $\mathcal{X}^s$  is compact, and  $\sup_{\mathbf{x} \in \mathcal{X}^s} |h^s(\mathbf{x})| < \infty$ . Equipped with Assumption (A.1), we have the following key result demonstrating the upper bound of  $R^t(h^t)$  in terms of  $R^s(h^s)$ .

**Theorem 2.** *Assume that Assumption (A.1) holds. Then, for any hypothesis  $h^s \in \mathcal{H}^s$ , the following inequality holds:*

$$\Delta R(h^s, h^t) \leq M (WS_{c_{0/1}}(\mathbb{P}^s, \mathbb{P}^\#) + \min\{\mathbb{E}_{\mathbb{P}^\#}[\|\Delta p(y | \mathbf{x})\|_1], \mathbb{E}_{\mathbb{P}^s}[\|\Delta p(y | \mathbf{x})\|_1]\}),$$

where  $\Delta p(y | \mathbf{x})$  is given by  $\Delta p(y | \mathbf{x}) := p^t(y | T_{st}(\mathbf{x})) - p^s(y | \mathbf{x})$ , and  $WS_{c_{0/1}}(\cdot, \cdot)$  is the Wasserstein distance with respect to the cost function  $c_{0/1}(\mathbf{x}, \mathbf{x}') = \mathbf{1}_{\mathbf{x} \neq \mathbf{x}'}$ , which returns 1 if  $\mathbf{x} \neq \mathbf{x}'$  and 0 otherwise.

*Remark 3.* If the following assumptions hold:

- (i) The transformation mapping  $T_{st}(\mathbf{x}) = \mathbf{x}$ , i.e., we use the same hypothesis set for both the source and target domains,
- (ii) The loss  $\ell(y, h(\mathbf{x})) = \frac{1}{2} |y - h(\mathbf{x})|$  where we restrict to consider hypothesis  $h : \mathcal{X} \rightarrow \{-1, 1\}$ ,

then we recover Theorem 1 in [2].

*Remark 4.* When  $WS_{c_{0/1}}(\mathbb{P}^s, \mathbb{P}^\#) = 0$  (i.e.,  $(T_{ts})_\# \mathbb{P}^t = \mathbb{P}^s$  or  $(T_{st})_\# \mathbb{P}^s = \mathbb{P}^t$ ), and there is a harmony between two supervisors of source and target domains (i.e.,  $p^s(y | \mathbf{x}) = p^t(y | T_{st}(\mathbf{x}))$ ), Theorem 2 suggests that we can do a perfect transfer learning without loss of performance. This fact is summarized in the following corollary.

**Corollary 5.** *Assume that  $(T_{ts})_\# \mathbb{P}^t = \mathbb{P}^s$  (or equivalently  $(T_{st})_\# \mathbb{P}^s = \mathbb{P}^t$ ) and the source and target supervisor distributions are harmonic in the sense that  $p^s(y | \mathbf{x}) = p^t(y | T_{st}(\mathbf{x}))$  (or equivalently  $p^t(y | \mathbf{x}) = p^s(y | T_{ts}(\mathbf{x}))$ ). Then, we can do a perfect transfer learning between the source and target domains.*

## 2.2 Optimization via Wasserstein metric

Corollary 5 suggest that we can do a perfect transfer learning from the source to target domains if we can point out a bijective map that transports the target to source distributions and two supervisor distributions are harmonic via this map. This is consistent with what is achieved in Theorem 2 for which the upper bound of the loss variance  $\Delta R(h^s, h^t)$  vanishes. Particularly, the upper bound in Theorem 2 consists of two terms wherein the first term quantifies how distant the transport and source domains and the second term relates to the discrepancy of two supervisor distributions. Still, from Theorem 2, we obtain the following inequality:

$$R^t(h_t) \leq R^s(h_s) + M \left( \text{WS}_{c_{0/1}}(\mathbb{P}^s, \mathbb{P}^\#) + \min \{ \mathbb{E}_{\mathbb{P}^\#} [\|\Delta p(y | \mathbf{x})\|_1], \mathbb{E}_{\mathbb{P}^s} [\|\Delta p(y | \mathbf{x})\|_1] \} \right),$$

which requires us to find the best hypothesis  $h_s^*$  and transformation  $T_{ts}^*$  for minimizing the general loss  $R^s(h_s)$  and the remaining term. To minimize the remaining term, due to the lack of target labels, it is natural to focus on minimizing the first term  $\text{WS}_{c_{0-1}}(\mathbb{P}^s, \mathbb{P}^\#)$  by restricting the transformation  $T_{ts}$  in the family of those what can transport the target to source distributions. By this restriction, the problem of interest boils down to answering the question: *among the bijective maps  $T_{ts}$  that transport the target to source distributions which transformation incurs the minimal discrepancy as specified in the second term of the upper bound in Theorem 2.*

We further tackle the task of finding the bijective maps that transport the target to source distributions via the Wasserstein distance with respect to the cost function (or metric)  $c$  and  $p > 0$  as:

$$\min_H \text{WS}_{c,p}(H_\# \mathbb{P}^t, \mathbb{P}^s), \quad (1)$$

where  $\text{WS}_{c,p}(\mathbb{P}, \mathbb{Q}) = \inf_{T_{\#} \mathbb{P}=\mathbb{Q}} \mathbb{E}_{\mathbf{x} \sim \mathbb{P}} [c(\mathbf{x}, T(\mathbf{x}))^p]^{1/p}$  is a Wasserstein distance between two distributions  $\mathbb{P}$  and  $\mathbb{Q}$ .

Let  $\mathcal{Z}$  be an intermediate space (i.e., the joint space  $\mathcal{Z} = \mathbb{R}^m$ ). We consider the composite mappings  $H: H(\mathbf{x}) = H^2(H^1(\mathbf{x}))$  where  $H^1$  is an injective mapping from the target domain  $\mathcal{X}^t$  to the joint space  $\mathcal{Z}$  and  $H^2$  maps from the joint space  $\mathcal{Z}$  to the source domain  $\mathcal{X}^s$  (note that if  $\mathcal{Z} = \mathcal{X}^s$  then  $H^2 = id$  is the identity function). Based on that structure on  $H$ , we can recast the optimization with Wasserstein metric in (1) into the following optimization problem:

$$\min_{H^1, H^2} \text{WS}_{c,p} \left( (H^2 \circ H^1)_\# \mathbb{P}^t, \mathbb{P}^s \right). \quad (2)$$

In the following theorem, we demonstrate that the above optimization problem can be equivalently transformed into another form involving the joint space (see Figure 1 for an illustration of that theorem).

**Theorem 6.** *The optimization problem (2) is equivalent to the following optimization problem:*

$$\min_{H^1, H^2} \min_{G^1: H^1_\# \mathbb{P}^t = G^1_\# \mathbb{P}^s} \mathbb{E}_{\mathbf{x} \sim \mathbb{P}^s} \left[ c(\mathbf{x}, H^2(G^1(\mathbf{x})))^p \right]^{1/p}, \quad (3)$$

where  $G^1$  is an injective map from the source domain  $\mathcal{X}^s$  to the joint space  $\mathcal{Z}$ .

It is interesting to interpret  $G^1$  and  $H^1$  as two generators that map the source and target domains to the common joint space  $\mathcal{Z}$  respectively. The constraint  $H^1_\# \mathbb{P}^t = G^1_\# \mathbb{P}^s$  further indicates that the gap between the source and target distributions is closed in the joint space via two generators  $G^1$  and  $H^1$ . Furthermore,  $H^2$  maps from the joint space to the source domain and aims to reconstruct  $G^1$ , hence ensuring  $G^1$  to be injective. Similar to [20], we do relaxation and arrive at the optimization problem:

$$\min_{H^1, H^2, G^1} \left( \mathbb{E}_{\mathbf{x} \sim \mathbb{P}^s} \left[ c(\mathbf{x}, H^2(G^1(\mathbf{x})))^p \right]^{1/p} + \alpha D(G^1_\# \mathbb{P}^s, H^1_\# \mathbb{P}^t) \right), \quad (4)$$

where  $D(\cdot, \cdot)$  specifies a divergence between two distributions over the joint space and  $\alpha > 0$ .

It is obvious that when the trade-off parameter  $\alpha$  approaches  $+\infty$ , the solution of the relaxation problem in Eq. (4) approaches the optimal solution in Eq. (3). Moreover, we add another reconstruction term to ensure the injection of  $H^1$  and come with the optimization problem:

$$\min_{H^1:2, G^1:2} \left( \mathbb{E}_{\mathbb{P}^s} \left[ c(\mathbf{x}, H^2(G^1(\mathbf{x})))^p \right]^{1/p} + \mathbb{E}_{\mathbb{P}^t} \left[ c(\mathbf{x}, G^2(H^1(\mathbf{x})))^p \right]^{1/p} + \alpha D(G^1_\# \mathbb{P}^s, H^1_\# \mathbb{P}^t) \right). \quad (5)$$

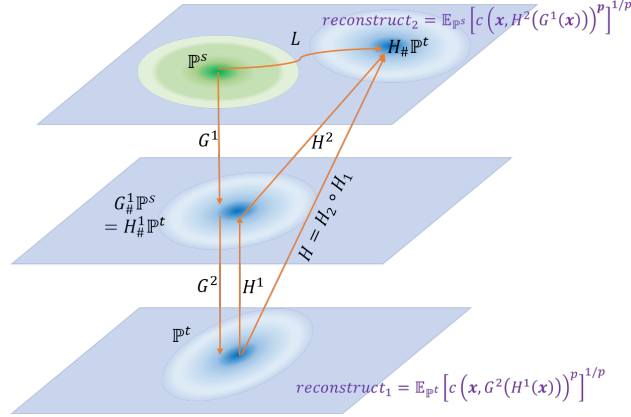


Figure 1: Theoretical view of Deep Domain Adaptation. The mapping  $H = H^2 \circ H^1$  maps from the target to source domains, while the mapping  $G = G^2 \circ G^1$  maps from the source to target domains. We minimize  $D(G^1_{\#} \mathbb{P}^s, H^1_{\#} \mathbb{P}^t)$  to close the discrepancy gap of the source and target domains in the joint space. In addition, we further minimize the reconstruction terms to avoid the mode collapse. Interestingly, our formulation has a strong connection to unsupervised style transfer (e.g., CycleGAN [24], DiscoGAN [12]).

To enable the transfer learning, we can train a supervised classifier  $\mathcal{C}$  on either  $\mathcal{D}^s = \{(\mathbf{x}_1^s, y_1), \dots, (\mathbf{x}_{N_s}^s, y_s)\}$  or  $G^1(\mathcal{D}^s) = \{(G^1(\mathbf{x}_1^s), y_1), \dots, (G^1(\mathbf{x}_{N_s}^s), y_s)\}$ . The final optimization problem is hence as follows:

$$\min_{H^{1:2}, G^{1:2}} \left( \mathbb{E}_{\mathbf{x} \sim \mathbb{P}^s} \left[ c(\mathbf{x}, H^2(G^1(\mathbf{x})))^p \right]^{1/p} + \mathbb{E}_{\mathbf{x} \sim \mathbb{P}^t} \left[ c(\mathbf{x}, G^2(H^1(\mathbf{x})))^p \right]^{1/p} \right. \\ \left. + \alpha D(G^1_{\#} \mathbb{P}^s, H^1_{\#} \mathbb{P}^t) + \beta \mathbb{E}_{(\mathbf{x}, y) \sim \mathcal{D}^s} [\ell(y, \mathcal{C}(A(\mathbf{x})))] \right), \quad (6)$$

where  $A$  is either the identity map (if we train the classifier  $\mathcal{C}$  on  $\mathcal{D}^s$ ) or  $G^1$  (if we train the classifier  $\mathcal{C}$  on  $G^1(\mathcal{D}^s)$ ) and  $\beta > 0$ .

Since  $G^1$  and  $H^1$  are two injective maps from the source and target domains to the joint space, we can further define two source and target supervisor distributions on the joint space as  $p^{\#,s}(y | G^1(\mathbf{x})) = p^s(y | \mathbf{x})$  and  $p^{\#,t}(y | H^1(\mathbf{x})) = p^t(y | \mathbf{x})$ . With respect to the joint space, the second term of the upper bound in Theorem 2 can be rewritten as in the following corollary.

**Corollary 7.** *The second term of the upper bound in Theorem 2 can be rewritten as*

$$\min \left\{ \mathbb{E}_{\mathbb{P}^s} \left[ \left\| p^{\#,t}(y | G^1(\mathbf{x})) - p^{\#,s}(y | G^1(\mathbf{x})) \right\|_1 \right], \mathbb{E}_{\mathbb{P}^t} \left[ \left\| p^{\#,t}(y | H^1(\mathbf{x})) - p^{\#,s}(y | H^1(\mathbf{x})) \right\|_1 \right] \right\}.$$

It is worth noting that solving the optimization problem (6) is only a part of the problem of interest since although the optimal map  $H = H^2 \circ H^1$  transports the target to source distributions, the discrepancy gap in labeling source and target domains is likely high. Moreover, Corollary 7 sheds light on when this discrepancy gap in labeling (the second term of the upper bound) is low or high, that is, this gap is low if  $G^1$  and  $H^1$  map the corresponding classes of the source and target domains together in the joint space and in contrast, this gap is high if there is a mismatch as mapping the corresponding classes to the joint space. In the experimental section, we design experiments to demonstrate these behaviors and how the harmony in these two labeling assignment mechanisms affects the predictive performance. In addition, two reconstruction terms in (6) contribute to preserve the clustering structures of source and target domains in the joint space, hence helps to reduce the mode collapsing problem. Finally, in deep domain adaption, we employ multilayered neural networks to formulate the transporting transformation  $H$  and the joint space specifies an intermediate layer in this this network.

**Further discussion.** Our formulation in Eq. (5) has a strong implication to unsupervised style transfer (e.g., CycleGAN [24] and DiscoGAN [12]) wherein one needs to learn a non-degenerate map that transports the source to target distributions. Our theory can mathematically explain what has been done in CycleGAN and DiscoGAN. In particular, the common formulation in CycleGAN [24] and

DiscoGAN [12] is in the spectrum of our (5) as we consider the L1 metric:  $c(\mathbf{x}, \mathbf{x}') = \|\mathbf{x} - \mathbf{x}'\|_1$  and set  $p = 1$ , and the joint (intermediate) layer is the last layer of  $H$  (i.e.,  $H^1(\mathbf{x}) = H(\mathbf{x})$ ,  $H^2(\mathbf{x}) = \mathbf{x}$ ) and the first layer  $G$  (i.e.,  $G^1(\mathbf{x}) = \mathbf{x}$ ,  $G^2(\mathbf{x}) = G(\mathbf{x})$ ). With this setting, our Eq. (5) reads:

$$\min_{H,G} \left( \mathbb{E}_{\mathbb{P}^t} [\|\mathbf{x} - G(H(\mathbf{x}))\|_1] + \alpha D(\mathbb{P}^s, H_{\#}\mathbb{P}^t) \right). \quad (7)$$

Compared with the formulation in CycleGAN [24] and DiscoGAN [12], Eq. (7) lacks of the opposite term:  $\mathbb{E}_{\mathbb{P}^s} [\|\mathbf{x} - H(G(\mathbf{x}))\|_1] + \alpha D(\mathbb{P}^t, G_{\#}\mathbb{P}^s)$ . However, this missing term can be introduced in our theory if we learn another transformation  $G$  that transports  $\mathbb{P}^s$  to  $\mathbb{P}^t$  via a Wasserstein distance.

### 3 Experiment

We conduct the experiments on the synthetic dataset to empirically verify our proposed theory and on the real-world datasets to demonstrate the influence of reconstruction terms and how harmony in two labeling assignment mechanisms affects the predictive performance. To bridge the gap between the source and target domains, inspired by [6], we employ GAN principle [8].

#### 3.1 Experiment on Synthetic Data

##### 3.1.1 Synthetic Dataset for the Source and Target Domains

We generate two synthetic labeled datasets for the source and target domains. We generate the 10,000 data examples of the source dataset from the mixture of two Gaussian distributions:  $p^s(\mathbf{x}) = \pi_1^s \mathcal{N}(\mathbf{x} | \boldsymbol{\mu}_1^s, \Sigma_1^s) + \pi_2^s \mathcal{N}(\mathbf{x} | \boldsymbol{\mu}_2^s, \Sigma_2^s)$  where  $\pi_1^s = \pi_2^s = \frac{1}{2}$ ,  $\boldsymbol{\mu}_1^s = [1, 1, \dots, 1] \in \mathbb{R}^{10}$ ,  $\boldsymbol{\mu}_2^s = [2, 2, \dots, 2] \in \mathbb{R}^{10}$  and  $\Sigma_1^s = \Sigma_2^s = \mathbb{I}_{10}$ . Similarly, we generate the another 10,000 data examples of the target dataset from the mixture of two Gaussian distributions:  $p^t(\mathbf{x}) = \pi_1^t \mathcal{N}(\mathbf{x} | \boldsymbol{\mu}_1^t, \Sigma_1^t) + \pi_2^t \mathcal{N}(\mathbf{x} | \boldsymbol{\mu}_2^t, \Sigma_2^t)$  where  $\pi_1^t = \frac{1}{3}$ ,  $\pi_2^t = \frac{2}{3}$ ,  $\boldsymbol{\mu}_1^t = [4, 4, \dots, 4] \in \mathbb{R}^{10}$ ,  $\boldsymbol{\mu}_2^t = [5, 5, \dots, 5] \in \mathbb{R}^{10}$  and  $\Sigma_1^t = \Sigma_2^t = \mathbb{I}_{10}$ . For each data example in the source and target domains, we assign label  $y = 0$  if this data example is generated from the first Gauss and  $y = 1$  if this data example is generated from the second Gauss using Bayes' s rule.

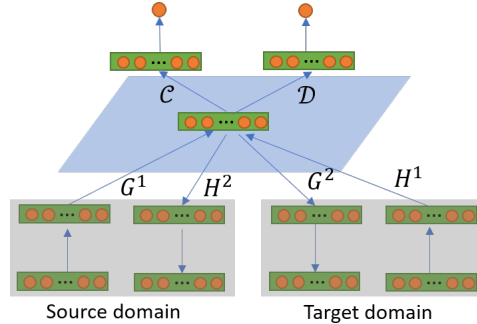


Figure 2: Architecture of networks for deep domain adaptation.

##### 3.1.2 Deep Domain Adaptation on the Synthetic Dataset

Figure 2 shows the architectures of networks used in our experiments on the synthetic datasets. Two generators  $G^1, H^1$  with the same architectures ( $10 \rightarrow 5$  (ReLU)  $\rightarrow 5$  (ReLU)) map the source and target data to the intermediate joint layer. Note that different from other works in deep domain adaptation, we did not tie  $G^1$  and  $H^1$ . Two other networks  $G^2, H^2$  with the same architectures ( $10 \rightarrow 5$  (ReLU)  $\rightarrow 5$  (ReLU)) map from the intermediate joint layer to the source and target domains respectively. The purpose of  $G^2, H^2$  is to reconstruct  $H^1, G^1$  respectively. To break the gap between the source and target domains in the joint layer, we employ GAN principle [8, 6] wherein we invoke a discriminator network  $\mathcal{D}$  ( $5 \rightarrow 5$  (ReLU)  $\rightarrow 1$  (sigmoid)) to discriminate the source and target data examples in the joint space. The classifier network  $\mathcal{C}$  ( $5 \rightarrow 5$  (ReLU)  $\rightarrow 1$  (sigmoid)) is employed to classify the labeled source data examples. To approximate the 0/1 cost function [16]:  $c_\gamma(\mathbf{x}, \mathbf{x}') = 2 / [1 + \exp\{-\gamma \|\mathbf{x} - \mathbf{x}'\|_2\}] - 1$  with  $\gamma = 100$ . It can be seen that when  $\gamma \rightarrow +\infty$ , the cost function  $c_\gamma$  approaches the 0/1 cost function. More specifically, we

need to update  $G^{1:2}$ ,  $H^{1:2}$ ,  $\mathcal{C}$ , and  $\mathcal{D}$  as follows:

$$(G^{1:2}, H^{1:2}, \mathcal{C}) = \underset{G^{1:2}, H^{1:2}, \mathcal{C}}{\operatorname{argmin}} \mathcal{I}(G^{1:2}, H^{1:2}, \mathcal{C}) \text{ and } \mathcal{D} = \underset{\mathcal{D}}{\operatorname{argmax}} \mathcal{J}(\mathcal{D}),$$

where  $\alpha$  is set to 0.1 and we have defined

$$\begin{aligned} \mathcal{I}(G^{1:2}, H^{1:2}, \mathcal{C}) &= \mathbb{E}_{\mathbf{x} \sim \mathbb{P}^t} [c_\gamma(\mathbf{x}, G^2(H^1(\mathbf{x})))] \\ &+ \mathbb{E}_{\mathbf{x} \sim \mathbb{P}^s} [c_\gamma(\mathbf{x}, H^2(G^1(\mathbf{x})))] + \mathbb{E}_{(\mathbf{x}, y) \sim \mathcal{D}^s} [\ell(y, \mathcal{C}(G(\mathbf{x})))] \\ &+ \alpha [\mathbb{E}_{\mathbf{x} \sim \mathbb{P}^s} [\log(\mathcal{D}(G(\mathbf{x})))]] + \mathbb{E}_{\mathbf{x} \sim \mathbb{P}^t} [\log(1 - \mathcal{D}(G(\mathbf{x})))]] \\ \mathcal{J}(\mathcal{D}) &= \mathbb{E}_{\mathbf{x} \sim \mathbb{P}^s} [\log(\mathcal{D}(G(\mathbf{x})))]] + \mathbb{E}_{\mathbf{x} \sim \mathbb{P}^t} [\log(1 - \mathcal{D}(G(\mathbf{x})))]. \end{aligned}$$

Based on the classifier  $\mathcal{C}$  on the joint space, we can identify the corresponding hypotheses on the source and target domains as:  $h^s(\mathbf{x}) = \mathcal{C}(G(\mathbf{x}))$  and  $h^t(\mathbf{x}) = \mathcal{C}(H(\mathbf{x}))$ .

### 3.1.3 Verification of Our Theory for Unsupervised Domain Adaptation

In this experiment, we assume that none of data example in the target domain has label. We measure three terms, namely  $|R(h^t) - R(h^s)|$ ,  $WS(\mathbb{P}^s, \mathbb{P}^\#)$ , and  $\min\{\mathbb{E}_{\mathbb{P}^\#} [\|\Delta p(y | \mathbf{x})\|_1], \mathbb{E}_{\mathbb{P}^s} [\|\Delta p(y | \mathbf{x})\|_1]\}$  ( $M = 1$  since we are using the logistic loss) as defined in Theorem 2 across the training progress. Actually, we approximate  $R(h^t)$ ,  $R(h^s)$  using the corresponding empirical losses. As shown in Figure 3 (middle), the green plot is always above the blue plot and this empirically confirms the inequality in Theorem 2. Furthermore, the fact that three terms consistently decrease across the training progress indicates an improvement when  $\mathbb{P}^\#$  is shifting toward  $\mathbb{P}^s$ . This improvement is also reflected in Figure 3 (left and right) wherein the target accuracy and empirical loss gradually increase and decrease accordingly.

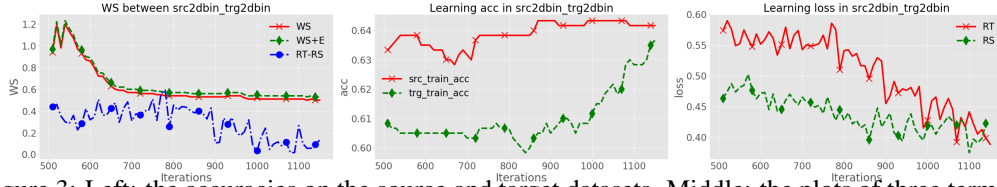


Figure 3: Left: the accuracies on the source and target datasets. Middle: the plots of three terms in Theorem 2. Right: the plot of empirical losses on the source and target datasets.

## 3.2 Experiment on Real-world Datasets

We conduct the experiments on the real-world datasets to demonstrate the effect of the reconstruction term to the predictive performance and also the behaviors when the transport transformation  $T_{ts}$  causes the match or mismatch of two labeling assignment mechanisms in the joint space (i.e., we properly and improperly align the classes of two domains in the joint space). It is worth noting that we do not seek the state-of-the-art performance in our experiments. Alternatively, we only focus on investigating the behaviors of the additional theoretical components. Bearing this in mind, we base on the relevant architectures and experimental protocols in [6] and then start adding the additional components.

### 3.2.1 The Effect of The Reconstruction Term

As mentioned before, we make use of the relevant architectures for the generators  $G^1, H^1$ , the discriminator  $\mathcal{D}$ , and the domain classifier  $\mathcal{C}$  as proposed in [6] and then add additional components  $G^2, H^2$  for the reconstruction terms. Note that unlike [6] and other works, we do not tie the parameters of two generators  $G^1$  and  $H^1$ . We always tie the parameters of  $G^1, H^2$  and  $H^1, G^2$  because they are encoders and decoders which aim to reconstruct source and target samples respectively. Moreover, we slightly modify Eq. (6) by setting the hyper-parameter  $\beta$  to 1 and introducing  $\theta > 0$  as the hyper-parameter of the reconstruction terms. The hyper-parameter  $\alpha$  (corresponding to the adaptation factor  $\lambda$  in [6]) is scheduled as proposed in that paper. Finally, we search  $\theta$  in the grid  $\{0.2, 0.4, 0.6, 0.8, 1\}$  and obtain the following experimental results.

In the experimental results in Table (1), for the first pair, the predictive performance starts increasing, peaks at its maximum, and then drops, whereas the predictive performance for the second pair peaks at  $\theta = 0$  (i.e., no reconstruction term). This shows that preserving the geometry/cluster structure of the

$\theta$	Our Model					DANN[6]
	$\theta = 0.2$	$\theta = 0.4$	$\theta = 0.6$	$\theta = 0.8$	$\theta = 1.0$	$\theta = 0$
<b>MNIST</b> → <b>MNIST-M</b>	81.7	83.2	<b>88.7</b>	85.6	80.2	81.5
<b>SVHN</b> → <b>MNIST</b>	68.4	67.8	64.4	62.8	61.3	<b>71.0</b>

Table 1: The variation of predictive performance in percentage when adding the reconstruction terms. Note that as  $\theta = 0$ , our model coincides DANN in [6]. We emphasize in bold the best performance.

source/target domains in the joint space is an ingredient that helps improve the predictive performance and avoid the mode collapse, but might cause the source and target examples harder to mix up in the joint space because this adds more constraint to this process (e.g., there is no improvement for the second pair). In practice, we can tweak this corresponding trade-off parameter to partly preserving the geometry/cluster structures in the original spaces whereas making it convenient for mixing up the source and target examples in the joint space.

### 3.2.2 The Effect of Class Alignment in the Joint Space

In this experiment, we inspect the influence of the harmony of two labeling assignment mechanisms to the predictive performance. In particular, we assume that a portion ( $r = 5\%, 15\%, 25\%, 50\%$ ) of the target domain has label and consider two settings: i) the labels of the target and source domains are totally properly matched in the joint space (i.e., 0 matches 0, 1 matches 1, ..., and 9 matches 9) and ii) the labels of the target and source domains are totally improperly matches in the joint space (i.e., 0 matches 1, 1 matches 2, ..., and 9 matches 0).

To push a specific labeled portion of the target domain to the corresponding label portion of the source domain in the joint space (the label  $i$  to  $i$  in the first setting and the label  $i$  to  $(i + 1) \bmod 10$  in the second setting for  $i = 0, 1, \dots, 9$ ), we again make use of GAN principle and employ additional discriminators to push the corresponding labeled portions together. Note that the parameters of the additional discriminators and the primary discriminator (used to push the target data toward source data in the joint space) are tied up to the penultimate layer.

$r$	Proper match				Improper match				Base
	5%	15%	25%	50%	5%	15%	25%	50%	0%
<b>MNIST</b> → <b>MNIST-M</b>	86.4	88.8	92.9	<b>93.2</b>	75.5	70.2	64.5	58.4	81.5
<b>SVHN</b> → <b>MNIST</b>	72.3	74.1	76.2	<b>77.5</b>	69.8	60.8	55.8	56.4	71.0

Table 2: The variation of predictive performance in percentage as increasing the ratio of labeled portion when the labels of the target domain are properly or improperly matched to those in the source domain. Note that we emphasize in bold and italic the best and worse performance.

It can be observed from the experimental results in Table (2) that for the case of proper matching, when increasing the ratio of labeled portion, we increase the chance to match the corresponding labeled portions properly, hence significantly improving the predictive performance. In contrast, for the case of improper matching, when increasing the ratio of labeled portion, we increase the chance to match the corresponding labeled portions improperly, hence significantly reducing the predictive performance.

## 4 Conclusion

Deep domain adaptation is a recent powerful learning framework which aims to address the problem of scarcity of qualified labeled data for supervised learning. To enable transferring the learning across the source and target domains, deep domain adaptation tries to bridge the gap between the source and target distributions in a joint feature space. Although this idea is powerful and has empirically demonstrated its success in several recent work, its theoretical underpinnings are lacking and limited. In this paper, we have developed a rigorous theory to establish a firm theoretical foundation for deep domain adaptation. Our theory provides a much more stronger theoretical results with more realistic assumption for real-world applications compared with existing work. Our result further offers a theoretical explanation behind the rationale for deep domain adaptation approach in bridging the gap between the source and target domains in a joint space. Interestingly, our work provides a deep connection to unsupervised style transfer where popular models such as CycleGAN and DiscoGAN can be rigorously explained. Lastly, the merit of our work was further validated via extensive experiments.



## References

- [1] M. Baktashmotlagh, M. T. Harandi, B. C. Lovell, and M. Salzmann. Unsupervised domain adaptation by domain invariant projection. In *2013 IEEE International Conference on Computer Vision*, pages 769–776, Dec 2013.
- [2] S. Ben-David, J. Blitzer, K. Crammer, A. Kulesza, F. Pereira, and J. W. Vaughan. A theory of learning from different domains. *Mach. Learn.*, 79(1-2):151–175, May 2010.
- [3] K. M. Borgwardt, A. Gretton, M. J. Rasch, H.-P. Kriegel, B. Schölkopf, and A. J. Smola. Integrating structured biological data by kernel maximum mean discrepancy. *Bioinformatics*, 22(14):e49–e57, July 2006.
- [4] N. Courty, R. Flamary, D. Tuia, and A. Rakotomamonjy. Optimal transport for domain adaptation. *IEEE transactions on pattern analysis and machine intelligence*, 39(9):1853–1865, 2017.
- [5] G. French, M. Mackiewicz, and M. Fisher. Self-ensembling for visual domain adaptation. In *International Conference on Learning Representations*, 2018.
- [6] Y. Ganin and V. Lempitsky. Unsupervised domain adaptation by backpropagation. In *Proceedings of the 32nd International Conference on International Conference on Machine Learning - Volume 37, ICML’15*, pages 1180–1189, 2015.
- [7] B. Gong, K. Grauman, and F. Sha. Connecting the dots with landmarks: Discriminatively learning domain-invariant features for unsupervised domain adaptation. In Sanjoy Dasgupta and David McAllester, editors, *Proceedings of the 30th International Conference on Machine Learning*, volume 28 of *Proceedings of Machine Learning Research*, pages 222–230, Atlanta, Georgia, USA, 17–19 Jun 2013.
- [8] Ian Goodfellow, Jean Pouget-Abadie, Mehdi Mirza, Bing Xu, David Warde-Farley, Sherjil Ozair, Aaron Courville, and Yoshua Bengio. Generative adversarial nets. In *Advances in neural information processing systems*, pages 2672–2680, 2014.
- [9] R. Gopalan, R. Li, and R. Chellappa. Domain adaptation for object recognition: An unsupervised approach. In *Proceedings of the 2011 International Conference on Computer Vision, ICCV ’11*, pages 999–1006, Washington, DC, USA, 2011. IEEE Computer Society.
- [10] A. Gretton, K. M. Borgwardt, M. Rasch, B. Schölkopf, and A. J. Smola. A kernel method for the two-sample-problem. In *Advances in neural information processing systems*, pages 513–520, 2007.
- [11] Jiayuan Huang, Arthur Gretton, Karsten M. Borgwardt, Bernhard Schölkopf, and Alex J. Smola. Correcting sample selection bias by unlabeled data. In B. Schölkopf, J. C. Platt, and T. Hoffman, editors, *Advances in Neural Information Processing Systems 19*, pages 601–608. MIT Press, 2007.
- [12] T. Kim, M. Cha, H. Kim, J. K. Lee, and J. Kim. Learning to discover cross-domain relations with generative adversarial networks. In Doina Precup and Yee Whye Teh, editors, *Proceedings of the 34th International Conference on Machine Learning*, volume 70 of *Proceedings of Machine Learning Research*, pages 1857–1865, International Convention Centre, Sydney, Australia, 06–11 Aug 2017. PMLR.
- [13] M. Long, Y. Cao, J. Wang, and M. Jordan. Learning transferable features with deep adaptation networks. In F. Bach and D. Blei, editors, *Proceedings of the 32nd International Conference on Machine Learning*, volume 37 of *Proceedings of Machine Learning Research*, pages 97–105, Lille, France, 2015.
- [14] M. Long, H. Zhu, J. Wang, and M. I. Jordan. Deep transfer learning with joint adaptation networks. In *Proceedings of the 34th International Conference on Machine Learning - Volume 70, ICML’17*, pages 2208–2217, 2017.

- [15] Y. Mansour, M. Mohri, and A. Rostamizadeh. Domain adaptation with multiple sources. In D. Koller, D. Schuurmans, Y. Bengio, and L. Bottou, editors, *Advances in Neural Information Processing Systems 21*, pages 1041–1048. 2009.
- [16] T. Nguyen and S. Sanner. Algorithms for direct 0–1 loss optimization in binary classification. In *Proceedings of the 30th International Conference on Machine Learning*, volume 28 of *Proceedings of Machine Learning Research*, pages 1085–1093, Atlanta, Georgia, USA, 17–19 Jun 2013. PMLR.
- [17] S. J. Pan, I. W. Tsang, J. T. Kwok, and Q. Yang. Domain adaptation via transfer component analysis. In *Proceedings of the 21st International Joint Conference on Artificial Intelligence, IJCAI’09*, pages 1187–1192, San Francisco, CA, USA, 2009. Morgan Kaufmann Publishers Inc.
- [18] I. Redko, A. Habrard, and M. Sebban. Theoretical analysis of domain adaptation with optimal transport. In *Joint European Conference on Machine Learning and Knowledge Discovery in Databases*, pages 737–753, 2017.
- [19] R. Shu, H. Bui, H. Narui, and S. Ermon. A DIRT-t approach to unsupervised domain adaptation. In *International Conference on Learning Representations*, 2018.
- [20] I. O. Tolstikhin, O. Bousquet, S. Gelly, and B. Schölkopf. Wasserstein auto-encoders. *CoRR*, abs/1711.01558, 2018.
- [21] E. Tzeng, J. Hoffman, T. Darrell, and K. Saenko. Simultaneous deep transfer across domains and tasks. *CoRR*, 2015.
- [22] V. N. Vapnik. *The Nature of Statistical Learning Theory*. Springer, second edition, November 1999.
- [23] Y. Zhang, Y. Liu, M. Long, and M. I. Jordan. Bridging theory and algorithm for domain adaptation. *CoRR*, abs/1904.05801, 2019.
- [24] J-Y Zhu, T. Park, P. Isola, and A. A. Efros. Unpaired image-to-image translation using cycle-consistent adversarial networks. In *Proceedings of the IEEE international conference on computer vision*, pages 2223–2232, 2017.